Decay pathways of excited electronic states of Group IV tetrafluoro and tetrachloro molecular ions studied with synchrotron radiation

Lambert, I. R.; Mason, S. M.; Tuckett, R. P.; Hopkirk, A.

DOI:
10.1063/1.455019

Decay pathways of excited electronic states of Group IV tetrafluoro and tetrachloro molecular ions studied with synchrotron radiation

I. R. Lambert, S. M. Mason, and R. P. Tuckett
Department of Chemistry, University of Birmingham, P. O. Box 363, Birmingham B15 2TT, United Kingdom

A. Hopkirk
SERC Daresbury Laboratory, Warrington, Cheshire WA4 4AD, United Kingdom

(Received 4 April 1988; accepted 20 May 1988)

This paper describes experiments to probe the dynamics and decay pathways of the $\tilde{C}\,^2T_2$ and $\tilde{D}\,^2A_1$ excited electronic states of Group IV tetrahalide molecular ions MX_4^+ (M = C, Si, Ge; X = F, Cl) in the gas phase. Tunable vacuum UV radiation from a synchrotron source is used to ionize MX_4 into these electronic states of MX_4^+. Flouorescence from ions initially produced or from fragments is monitored undispersed by a suitable pm tube. When the synchrotron is operated cw, such synchrotron-induced fluorescence spectra give energy thresholds for fluorescence, and in favorable cases an estimate of the fluorescence quantum yield (of MX_4^+ $\tilde{C}$ or $\tilde{D}$) can be made. When the synchrotron is operated pulsed, radiative lifetimes can be measured as a function of excitation energy. The fluorides and chlorides display very different decay properties. The dynamical behavior of these states is rationalized (a) with respect to their spectroscopic properties, and (b) with respect to the dissociation channels energetically "open" to them.

I. INTRODUCTION

We have recently observed electronic emission spectra of several Group IV tetrafluoro and tetrachloro molecular ions MX_4^+ (M = C, Si, Ge; X = F, Cl) in the gas phase.[1-4] For the three fluorides CF_4^+, SiF_4^+, and GeF_4^+, both continuous and discrete bands have been observed in the UV to visible region of the electromagnetic spectrum. The spectra are observed at a low rotational temperature ($\sim$25 K) in a crossed molecular beam/electron beam apparatus.[1-3] The ground and first two excited state ($\tilde{X}$, $\tilde{A}$, and $\tilde{B}$) of these ions dissociate rapidly (to $MF_3^+ + F$), and the continuous bands arise from transitions to these states.[5-7] The discrete band arises from a transition between the fourth and third excited electronic states $\tilde{D}\,^2A_1$–$\tilde{C}\,^2T_2$, both of which are bound. This $\tilde{D}$–$\tilde{C}$ electronic spectrum of CF_4^+, SiF_4^+, and GeF_4^+ has been studied in great detail,[1-3] and computer simulation of the rotational band contours has confirmed that the observed vibronic bands are due to a $^2A_1$–$^2T_2$ transition of a tetrahedral molecule observed at a low rotational temperature.[8] These excited electronic states of the three chloride ions CCl_4^+, $SiCl_4^+$, and $GeCl_4^+$ show very different decay properties.[4] The $\tilde{D}$ state of these ions do not fluoresce, but decay nonradiatively. The $\tilde{C}$ state of $SiCl_4^+$ and $GeCl_4^+$ decays radiatively, whereas CCl_4^+ $\tilde{C}$ decays nonradiatively.

We believe that the most important aspect of this work is not the purely spectroscopic properties of these excited electronic states of MX_4^+. Our aim is to understand the dynamics of the decay pathways of the $\tilde{C}$ and $\tilde{D}$ states of MX_4^+. These states lie several eV above the lowest ionic dissociation channel (Sec. III of Ref. 4), and several other dissociation channels are energetically open. Such states might be expected to decay nonradiatively rather than radiatively, and the observation of fluorescence decay is therefore surprising. In this paper we describe experiments to measure threshold energies, fluorescence quantum yields $\phi_{h\nu}$, and radiative lifetimes of these fluorescing states of MX_4^+. Tunable vacuum UV radiation from the SERC Daresbury Synchrotron Source is used to ionize MX_4 into selected electronic states of MX_4^+, and fluorescence from the ions is collected undispersed by a suitable pm tube + filter. Two types of experiment are performed. First, the synchrotron is operated multibunch or quasi cw, and fluorescence spectra are recorded as a function of excitation energy. This experiment gives threshold energies at which a fluorescence channel "turns on," and can be used to determine the emitter of a particular fluorescence band system.[4] Furthermore, in favorable cases the fluorescence quantum yield of a particular electronic state of MX_4^+ can be estimated as a function of excitation energy. Second, the synchrotron is operated single bunch or in the pulsed mode (200 ps pulses every 320 ns on the Daresbury source). Radiative lifetimes of a fluorescing electronic state of MX_4^+ can then be measured as a function of excitation energy.

Section II describes the apparatus in detail, and how estimates of $\phi_{h\nu}$ can be made. Section III gives the energetics of the ionic states of MF_4 and their dissociation channels; the complementary information for the chlorides is given in Sec III of the previous paper.[4] Section IV describes the results of the synchrotron-excited fluorescence spectra for the three fluorides CF_4, SiF_4, and GeF_4; the complementary detailed information for MCl_4 is given in Sec. IV of Ref. 4. Section V describes the lifetime measurements, and some conclusions are made in Sec. VI.

II. EXPERIMENTAL

The experiments are performed in a stainless-steel chamber of 30 cm i.d. with eight identical ports arranged uniformly around the circumference. Gas is admitted to the chamber as a "spray" from a 0.2 mm i.d., 30 mm long stainless-steel needle mounted to a z translator on its top flange.

 0021-9606/88/172683-08$02.10

The bottom flange is connected to a 510 ℓs^{-1} turbo molecular pump, and the base pressure of the chamber $= 3\times10^{-8}$ Torr. With gas flowing, the background pressure is $\sim10^{-4}$ Torr, although the local pressure in the spray is substantially higher. The gas spray is crossed orthogonally by tunable synchrotron radiation dispersed from a 1 m vacuum UV Seya monochromator (pressure $= 10^{-9}$ Torr) equipped with a 1200 lines mm^{-1} grating blazed at 60 nm. Since we use wavelengths well below the LiF cutoff, a windowless system must be used. The synchrotron radiation from the exit slit of the Seya is therefore focused into a 2 mm i.d., 460 mm long glass capillary tube which ends approximately 5 mm from the crossing region with the gas spray. To minimize scattered light in the chamber, this tube is externally coated with black DAG. To protect the monochromator from MX_4 vapor, there is one stage of differential pumping (pumped by a 100 ℓs^{-1} turbo) between the exit slit of the Seya and the reaction chamber, and this region provides the mount for the glass capillary. The absolute synchrotron photon flux in the chamber is measured by an Al_2O_3 photocathode connected to a Keithley pico-ammeter and a voltage-to-frequency converter. Undispersed fluorescence from the $\tilde{C}$ or $\tilde{D}$ states of the MX_4^+ ions produced is focused by an $f/1.3$ concave mirror through a LiF window and a 50 mm square filter on to the photocathode of a photomultiplier tube. Two pm tube + filter combinations can be used so that fluorescence in two different spectral ranges can simultaneously be monitored (see Ref. 4). The signals are detected by single photon counting electronics.

Pure CF_4 and SiF_4 gas were supplied by BOC and Air Products, respectively, and were used without further purification. GeF_4 diluted in helium was prepared by the method described elsewhere.[3] The three chlorides are all liquids at room temperature, and were supplied by Aldrich Chemical Co. Their vapor pressure was admitted to the chamber from a glass container whose temperature was stabilized at 293 K.

In the multibunch or cw experiments, the resolution of the synchrotron radiation is 0.2 nm (i.e., 0.1 eV at 25 eV), and with the grating blazed at 60 nm (20.6 eV) the usable VUV photon range is 103–35 nm (i.e., 12–35 eV). Over this range the photon flux can vary by a factor of ~8, and hence it is essential to normalize the fluorescence signal to the photon flux at a particular excitation energy. The scanning of the Seya monochromator, the recording of the incident photon flux and fluorescence detection are computer controlled, and data is transferred to the Daresbury Mainframe Computer (AS7000) for analysis. In the pulsed experiments, the resolution of the monochromator is degraded to 0.5 nm to increase the (limited) photon flux in the single-bunch mode. Lifetime decays are collected by standard techniques using a time-to-amplitude converter and a multichannel analyzer. Decays are measured at different excitation energies. The data are transferred initially to the Daresbury Mainframe Computer, then to the University of Birmingham Mainframe (Honeywell DPS-8/70M) via the JANET network where they are analyzed using a multiexponential fitting procedure.

From the cw experiment, an estimate of the fluorescence quantum yield $\phi_{h\nu}$ can be made in the following way. We take $CF_4^+\,\tilde{C}\,^2T_2$ as an example. The number of $CF_4^+\,\tilde{C}$ ions produced per second per unit length is $p\cdot I_0\cdot\sigma$, where p is the gas spray pressure, I_0 is the incident photon flux, and σ is the partial ionisation cross section into $CF_4^+\,\tilde{C}$ at that particular excitation energy. If $\phi_{h\nu}$ is the fluorescence quantum yield of $CF_4^+\,\tilde{C}$, and only the $\tilde{C}$–$\tilde{A}$ fluorescence channel with branching ratio $BR_{h\nu}$ is detected with a collection efficiency $P_{h\nu}$, then the number of photons detected per second per unit length observed is $p\cdot I_0\cdot\sigma\cdot\phi_{h\nu}\cdot BR_{h\nu}\cdot P_{h\nu}$. To measure absolute quantum yields, therefore, the partial ionization cross section, the pressure in the spray, the path length in the interaction region and the photon collection efficiency of the pm tube must all be known. In practice, the apparatus is calibrated with N_2, measuring the photon count rate of N_2^+ B–X (0,0) emission at 391 nm through a narrow band interference filter when N_2 is excited with synchrotron radiation with energy above the $N_2^+\,B\,^2\Sigma_u^+$ threshold of 18.7 eV. The partial ionization cross section and the fluorescence branching ratio of the (0,0) band are known,[9] and $\phi_{h\nu}$ ($N_2^+\,B\,^2\Sigma_u^+$) is unity.[10] Thus knowing I_0 an estimate can be made of the product $p\cdot P_{h\nu}$. CF_4 at the same pressure as N_2 (as measured by a Penning gauge 15 cm from the spray) is admitted to the chamber, and it is assumed that $p\cdot P_{h\nu}$ is unchanged from its value with N_2. Measurement of $\phi_{h\nu}$ ($CF_4^+\,\tilde{C}$) then only needs a knowledge of the partial ionization cross section of CF_4 to $CF_4^+\,\tilde{C}$ and the branching ratio of the different fluorescence channels from $CF_4^+\,\tilde{C}$. Of the six Group IV tetrahalides studied, partial ionization cross sections are not known for GeF_4 and $GeCl_4$, and the SiF_4 data is limited. Furthermore, only an estimate of $\phi_{h\nu}$ can be made by this technique, since many approximations have to be made, and an error of $\pm$ 100% in a measurement is realistic. However, it is possible to measure the variation in $\phi_{h\nu}$ (rather than its absolute value) as a function of excitation energy with more accuracy.

III. ENERGETICS OF THE IONIC STATES OF MF_4 AND DISSOCIATION CHANNELS

The energies of the neutral and ionic dissociation channels of CCl_4, $SiCl_4$, and $GeCl_4$ have been given in Table I of the previous paper.[4] In this section we present the analogous information for the three fluorides. The valence molecular orbitals arise from overlap of the 16 fluorine atom valence orbitals F 2*s*,2*p* with the central atom orbitals (e.g., Si 3*s*,3*p*). The electron configuration corresponding to the five highest occupied molecular orbitals is $\cdots(2a_1)^2(2t_2)^6(1e)^4(3t_2)^6(1t_1)^6$, and again the core orbitals have been omitted in the numbering scheme. The first five electronic states of MX_4^+ have symmetry $\tilde{X}\,^2T_1$, $\tilde{A}\,^2T_2$, $\tilde{B}\,^2E$, $\tilde{C}\,^2T_2$, and $\tilde{D}\,^2A_1$, corresponding to electron removal from the $1t_1$, $3t_2$, $1e$, $2t_2$, and $2a_1$ molecular orbitals respectively, and the energies of these states are given in Table I. This photoelectron data is taken from Refs. 11–15. Since this paper is concerned with energy thresholds, we quote adiabatic ionization potentials (IPs) in the table, whereas the IPs quoted in Table I of Ref. 4 for the chlorides are vertical IPs.

Table I also shows the energies of the neutral and ionic dissociation channels of MF_4. The energies of the neutral

TABLE I. Energetics of dissociation channels of MF_4 and MF_4^+ (M = C,Si,Ge) in eV.

Neutral/parent ion	Dissociation channel	Energy (eV)[a]
	$CF + F^+ + F_2$	30.4
	$CF + F + F_2^+$	28.7
$CF_4^+ \tilde{D}\,^2A_1$		25.12
	$CF_2 + F_2^+$	23.3
	$CF_3 + F^+$	22.9
	$CF^+ + F + F_2$	22.1
$\tilde{C}\,^2T_2$		21.70
	$CF_2^+ + F_2$	19.2
$\tilde{B}\,^2E$		18.30
$\tilde{A}\,^2T_2$		17.10
$CF_4^+ \tilde{X}\,^2T_1$		15.35
	$CF_3^+ + F$	14.7
	$CF + F + F_2$	13.0
	$CF_2 + F_2$	7.6
	$CF_3 + F$	5.5
$CF_4 \tilde{X}\,^1A_1$		0
	$SiF + F^+ + F_2$	34.7
	$SiF + F + F_2^+$	33.0
	$SiF_2 + F_2^+$	26.3
	$SiF^+ + F + F_2$	24.6
	$SiF_3 + F^+$	24.3
$SiF_4^+ \tilde{D}\,^2A_1$		21.55
	$SiF_2^+ + F_2$	21.4
$\tilde{C}\,^2T_2$		19.30
$\tilde{B}\,^2E$		18.0
	$SiF + F + F_2$	17.3
$\tilde{A}\,^2T_2$		17.3
	$SiF_3^+ + F$	16.2
$SiF_4^+ \tilde{X}\,^2T_1$		16.1
	$SiF_2 + F_2$	10.6
	$SiF_3 + F$	6.9
$SiF_4 \tilde{X}\,^1A_1$		0
	$GeF + F^+ + F_2$	32.3
	$GeF + F + F_2^+$	30.6
	$GeF_2 + F_2^+$	24.2
	$GeF_3 + F^+$	22.9
	$GeF^+ + F + F_2$	22.3
$GeF_4^+ \tilde{D}\,^2A_1$		21.3
	$GeF_2^+ + F_2$	20.3
$\tilde{C}\,^2T_2$		18.52
$\tilde{B}\,^2E$		17.01
$\tilde{A}\,^2T_2$		16.53
$GeF_4^+ \tilde{X}\,^2T_1$		16.06
	$GeF_3^+ + F$	15.7
	$GeF + F + F_2$	14.9
	$GeF_2 + F_2$	8.5
	$GeF_3 + F$	5.5
$GeF_4 \tilde{X}\,^1A_1$		0

[a] In addition to the thermodynamic and IP data in the text, we use IP (F_2) = 15.7 eV (Ref. 16), IP (F) = 17.4 eV (Ref. 17), and D^0 (F–F) = 1.6 eV (Ref. 18).

dissociation channels of MF_4. The energies of the neutral dissociation channels of CF_4 and SiF_4 come from direct measurements of heats of formation.[19,20] The energies of the GeF_4 channels come from indirect measurements, and are probably less accurate.[21] Direct IP measurements have been made for all the mono- and difluorides. Thus the adiabatic IP of CF is 9.1 eV,[22] SiF 7.3 eV,[23] GeF 7.4 eV,[24] CF_2 11.6 eV,[25] SiF_2 10.8 eV,[26] and GeF_2 11.8 eV.[27] The IP of CF_3 (9.2 eV[28]) comes from a direct measurement of the appearance potential of CF_3^+ from CF_3, and hence is an accurate value. Appearance potentials of SiF_3^+ and GeF_3^+ have only been measured from SiF_4 and GeF_4,[21,29] so the values for the IPs of SiF_3 and GeF_3 (9.3 and 10.2 eV, respectively) are approximate and represent an upper limit.

The $\tilde{D}\,^2A_1$ state of CF_4^+ has five ionic dissociation channels energetically open, yet this state decays radiatively (to lower-lying $\tilde{X}$, $\tilde{A}$, and $\tilde{C}$ states). The $\tilde{D}$ states of SiF_4^+ and GeF_4^+ both have two ionic channels open, yet again these states decay radiatively. However, as yet fluorescence quantum yields of MF_4^+ $\tilde{D}$ have not been measured, so it is not known how important these decay channels are. It is also not obvious from Table I why the $\tilde{C}\,^2T_2$ states of CF_4^+, SiF_4^+, and GeF_4^+ behave differently. SiF_4^+ and GeF_4^+ $\tilde{C}$ do not decay radiatively (Secs. IV B and IV C) with one ionic decay channel (to $SiF_3^+/GeF_3^+ + F$) open. Yet CF_4^+ $\tilde{C}$ fluoresce (Sec. IV A), even though two ionic channels (to $CF_3^+ + F$ and $CF_2^+ + F_2$) are now open.

IV. SYNCHROTRON-EXCITED FLUORESCENCE SPECTRA OF MX_4

A. CF_4

Figure 1 shows fluorescence spectra of CF_4 excited by synchrotron radiation in the range 21–31 eV. In Fig. 1(a) fluorescence in the region 250–390 nm is collected by an EMI 9883 QB photomultiplier tube + Schott UG11 filter, in Fig. 1(b) vacuum UV fluorescence in the region 120–200 nm is collected by an EMI CsI 9413 solar blind pm tube with no filter. Both tubes operate at room temperature. The fluorescence spectra have both been normalized to the photon flux, but their sensitivities are different. The 250–390 nm region overlaps most of the bound–free $\tilde{C}$–$\tilde{X}$ and $\tilde{C}$–$\tilde{A}$ bands of CF_4^+ (band centers 230 and 290 nm, respectively), the 120–200 nm region overlaps bound–free emission from the $\tilde{D}$ state of CF_4^+ ($\tilde{D}$–$\tilde{A}$ at 161 nm and $\tilde{D}$–$\tilde{B}$ at 187 nm).[5] The thresholds for fluorescence are measured to be 21.7 ± 0.1 and 25.0 ± 0.1 eV, respectively, in excellent agreement with the adiabatic IPs of the $\tilde{C}\,^2T_2$ and $\tilde{D}\,^2A_1$ states of CF_4^+ (Ta-

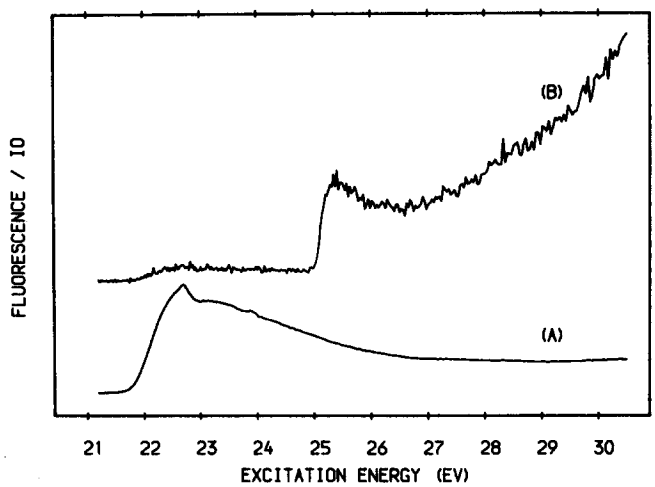

FIG. 1. Undispersed fluorescence of CF_4 excited by VUV radiation in the range 21–31 eV. In (a), UV fluorescence in the region 250–390 nm is collected; in (b), only vacuum UV fluorescence in the region 120–200 nm is collected. The photon count rates have been normalized to the synchrotron flux I_0. The scale of the normalized fluorescence axis is different in the two spectra.

ble I). The relative steepness of the $\tilde{D}$ state threshold to the $\tilde{C}$ state threshold is a Franck–Condon effect; ionization to $\tilde{D}\,^2A_1$ is a near vertical process with very little change in molecular geometry, whereas ionization to $\tilde{C}\,^2T_2$ involves a substantial change in the C–F bond distance with different adiabatic and vertical IPs.[8]

The total absorption cross section of CF_4 between 17 and 70 eV has been measured by Lee *et al.*,[30] and more recently partial ionisation cross sections (σ) of the five valence molecular orbitals of CF_4 have been measured in the same energy range by angle-resolved photoelectron spectroscopy.[31] For energies above threshold, the normalized fluorescence signal is proportional to the product $\phi_{h\nu}.\sigma$ (Sec. II). For $CF_4^+\,\tilde{C}$, σ increases from zero (at the threshold of 21.7 eV) to a maximum of 1.40×10^{-17} cm^2 at 24 eV, then decreases gradually to 0.64×10^{-17} cm^2 at 31 eV.[31] For $CF_4^+\,\tilde{D}$, σ increases sharply at its threshold to 5×10^{-19} cm^2 at 28 eV, then increases more gradually to 1.1×10^{-18} cm^2 at 31 eV.[31] These patterns are approximately observed in Figs. 1(a) and 1(b), respectively. Our experiments also complement the synchrotron-induced fluorescence spectra of CF_4 recently reported by Lee *et al.*[32] using the University of Wisconsin storage ring. They observed a turn on in a fluorescence decay channel at $\lambda = 57.4$ nm (21.6 eV corresponding to the adiabatic IP of $CF_4^+\,\tilde{C}$), but report no results for $\lambda < 50$ nm ($E > 24.8$ eV) so could not probe the $CF_4^+\,\tilde{D}$ state threshold. Lee *et al.* suggested that the probable emitter of the UV fluorescence was $CF_4^+\,\tilde{C}$, but an excited state of CF_3^+ (produced by rapid dissociation of $CF_4^+\,\tilde{C}$) was not ruled out.[32] The dispersed emission spectrum produced by fast ion beam bombardment of CF_4 at room temperature was also tentatively assigned to bound–free transitions in CF_4^+ by Aarts,[5] but again he could not completely rule out CF_3^+ as the emitter. We believe, however, that the combined evidence of the photoelectron data[11] and the threshold measurements reported here is so strong that the broad bands between 250–390 nm can definitely be assigned to $CF_4^+\,\tilde{C}$–$\tilde{X}$ and $\tilde{C}$–$\tilde{A}$, and the bands between 120–200 nm to $CF_4^+\,\tilde{D}$–$\tilde{A}$ and $\tilde{D}$–$\tilde{B}$ bound–free emission. The bound–bound $\tilde{D}$–$\tilde{C}$ band lies between 360 and 410 nm,[1,5] and will therefore be detected by the pm tube + filter combination in Fig. 1(a). However, we see no evidence for a second fluorescence threshold at 25.0 eV in Fig. 1(a), because the intensity of the $\tilde{C}$–$\tilde{X},\tilde{A}$ emission swamps the much weaker $\tilde{D}$–$\tilde{C}$ emission.

The EMI 9883 QB pm tube which detects $CF_4^+\,\tilde{C}$–$\tilde{X},\tilde{A}$ emission can also detect $N_2^+\,B$–X (0,0) emission at 391 nm. Using the method described in Sec. II we can estimate the fluorescence quantum yield of $CF_4^+\,\tilde{C}$ as a function of excitation energy. Partial ionization cross sections have been measured at eight energies between 21 and 36 eV.[31] We estimate $\phi_{h\nu}$ to be 0.5 at 23 eV, falling to 0.3_5 at 26 eV, then rising again to 0.4 at 31 eV. Due to the many approximations made, the uncertainty in these numbers is as high as a factor of 2. However, the relative values are more accurate, and in particular we believe the drop in $\phi_{h\nu}$ by $\sim$30% as the excitation energy rises to 26 eV (4.3 eV above threshold) is a genuine result (see also Sec. V A). Our values agree approximately with those of Lee *et al.*[32] who measure $\phi_{h\nu}$ to be 1.3 at 23 eV (53.9 nm) falling to 1.0 at 25 eV (49.6 nm)[41]; again, an uncertainty of a factor of 2 is quoted. It is thus clear that radiative decay of $CF_4^+\,\tilde{C}$ is a major decay pathway with $\phi_{h\nu}$ probably lying between 0.5 and its maximum value of 1. The fluorescence quantum yield of $CF_4^+\,\tilde{D}\,^2A_1$ cannot be measured in our experiment, because the efficiency of the EMI 9413 CsI solar blind pm tube cannot be calibrated with $N_2^+\,B$–X fluorescence.

B. SiF_4

Figure 2 shows the fluorescence spectrum of SiF_4 excited by VUV radiation in the range 21–36 eV. Fluorescence in the region 250–390 nm is collected by the EMI 9883 QB pm tube + Schott UG 11 filter. This region overlaps the bound–free $\tilde{D}$–$\tilde{A}$ and $\tilde{D}$–$\tilde{B}$ bands of SiF_4^+[6] with band centers at 304 and 370 nm, respectively. A sharp turn on in the fluorescence is observed at 21.5 ± 0.1 eV, in excellent agreement with the adiabatic IP of $SiF_4^+\,\tilde{D}\,^2A_1$ of 21.55 eV.[13] As with $CF_4^+\,\tilde{D}$, the rise is steep because ionization of SiF_4 to $SiF_4^+\,\tilde{D}$ is a near vertical process with little change in geometry.[8] The normalized fluorescence signal drops to a minimum at 28 eV, then rises between 28 and 36 eV. Fluorescence is collected simultaneously in the range 505–750 nm (cooled Mullard 2254 pm tube with an S20 photocathode + Schott OG515 filter), corresponding to $SiF_4^+\,\tilde{D}$–$\tilde{C}$ emission (band center 551 nm[2]); the fluorescence spectrum is identical to Fig. 2.

As for $CF_4^+\,\tilde{C}$, by calibration of the EMI 9883 QB tube (which detects $SiF_4^+\,\tilde{D}$–$\tilde{A},\tilde{B}$ emission) with $N_2^+\,B$–X fluorescence, the data can be used to estimate the fluorescence quantum yield $\phi_{h\nu}$ of $SiF_4^+\,\tilde{D}$. Branching ratios into the five valence ionic states of SiF_4^+ have been measured in the energy range 21–100 eV,[33] but the total absorption cross section has only been measured for $\lambda > 50$ nm ($E < 25$ eV).[34] Thus partial ionization cross sections into $SiF_4^+\,\tilde{D}$ can be calculated for six energies in the limited range 22–25 eV. By the method described in Sec. IV A, we estimate $\phi_{h\nu}(SiF_4^+\,\tilde{D})$ to be 0.6 and independent of energy. An error of a factor of 2 is realistic. This agrees with Lee *et al.*'s[34] recent report of synchrotron-induced fluorescence spectra of SiF_4 between 50 and 100 nm. They observe the same sharp turn on in fluorescence at 21.5 eV ($\lambda = 57.6$ nm), and estimate $\phi_{h\nu}$ of the fluorescing state ($SiF_4^+\,\tilde{D}$) to be 1.0 in the range 22–25

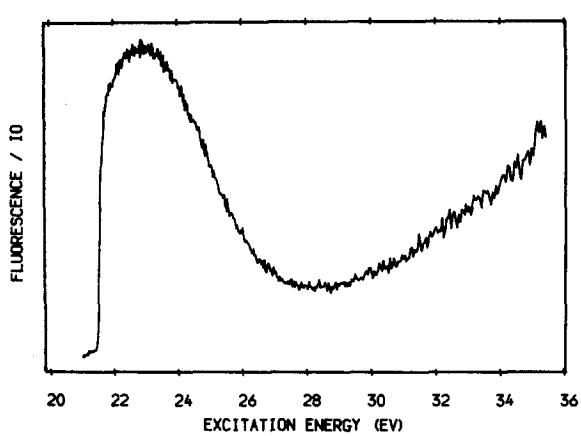

FIG. 2. Undispersed fluorescence of SiF_4 excited by VUV radiation in the range 21–36 eV. Only photons in the range 250–390 nm are collected, and the photon count rate has been normalized to the synchrotron flux I_0.

eV[41] (Fig. 2 of Ref. 34). Thus radiative decay is the major decay pathway of $SiF_4^+ \tilde{D}$, and despite being energetically open (Table I) the nonradiative channel to ionic fragment(s) is not operative.

We have also investigated the decay dynamics of the $\tilde{C}\,^2T_2$ state of SiF_4^+. If this state decays radiatively to lower-lying $\tilde{X}\,^2T_1$ and $\tilde{A}\,^2T_2$ states, then from photoelectron data[12] $\tilde{C}$–$\tilde{X}$ and $\tilde{C}$–$\tilde{A}$ fluorescence is expected to occur around 387 and 620 nm, respectively. However, no turn on in fluorescence in any wavelength region between 200 and 750 nm is observed when the VUV radiation is tuned through the energy of the $\tilde{C}$ state adiabatic IP (19.30 eV). Thus $SiF_4^+ \tilde{C}$ does not decay radiatively, or if it does its quantum yield is too low to be measured. Lee *et al.*[34] have obtained the same result. Furthermore, we have established that the broad band fluorescence around 610 nm, observed initially in the molecular beam/electron beam experiment and assigned to $SiF_4^+ \tilde{C}$–$\tilde{A}$,[2] is in fact due to emission from $SiF_4^+ \tilde{D}$. When fluorescence is detected only in the region 600–750 nm (Mullard 2254 pm tube + Schott OG610 filter) the fluorescence spectrum is identical to Fig. 2, i.e., fluorescence turns on at the $\tilde{D}$ state adiabatic IP. Thus the emitter of the broad band at 610 nm is $SiF_4^+ \tilde{D}$, and the lower state of the fluorescence can only be high lying, dissociative vibrational levels of $\tilde{C}$. van Lonkhuyzen and Aarts[7] have suggested that the higher vibrational levels of $\tilde{C}$ might be dissociative (while the lower levels clearly are not[2]) if a dissociation limit lies within the $\tilde{C}$ vibrational manifold. However, from Table I no dissociation channel around 19.5 eV exists.

C. GeF_4

Figure 3 shows fluorescence spectra of GeF_4 excited by VUV radiation in the range 21–26 eV. In Fig. 3(a), UV fluorescence in the region 240–390 nm is collected by a cooled Mullard 2020Q pm tube + Schott UG5 filter, in Fig. 3(b) visible fluorescence in the region 370–550 nm is collected by the uncooled EMI 9883 QB pm tube + Oriel LF38 cut-on filter. The former region overlaps the bound–free $\tilde{D}$–$\tilde{A}$ and $\tilde{D}$–$\tilde{B}$ bands of GeF_4^+ (band centers 255 and 290 nm[7]), the latter region the bound–bound $\tilde{D}$–$\tilde{C}$ band (band center 399 nm[3]). The spectra show the same threshold for fluorescence at 21.3 ± 0.1 eV in excellent agreement with the adiabatic IP of $GeF_4^+ \tilde{D}\,^2A_1$ of 21.3 eV.[15] Both spectra also show additional structure above the $\tilde{D}$ state threshold between 24.0 and 24.5 eV. When UV fluorescence is collected [Fig. 3(a)] two peaks are observed at 24.02 and 24.44 eV in the approximate intensity ratio 1:2. When visible fluorescence is collected [Fig. 3(b)] only the stronger peak at 24.44 eV is observed. The Seya monochromator was scanned up to 36 eV, but no additional structure is observed. Since the $\tilde{D}$ state of GeF_4^+ arises from electron removal from the lowest valence molecular orbital of GeF_4, it is unlikely that these peaks are due to Rydberg states of GeF_4. Furthermore, we have no explanation for why an extra peak (at 24.02 eV) is observed when fluorescence is collected in the UV rather than the visible. Neither total absorption cross sections nor partial ionization cross sections have been measured for

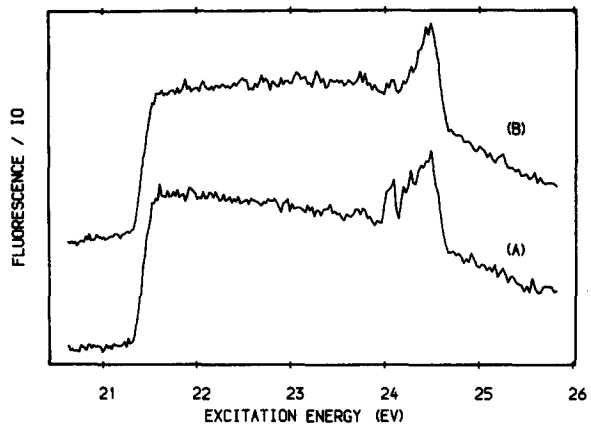

FIG. 3. Undispersed fluorescence of GeF_4 excited by VUV radiation in the range 21–26 eV. In (a), UV fluorescence in the range 240–390 nm is collected; in (b), only visible fluorescence in the range 370–550 nm is collected. The photon count rates have been normalized to the synchrotron photon flux I_0. The scale of the normalized fluorescence axis is different in the two spectra.

GeF_4, so it is not possible to estimate the fluorescence quantum yield $\phi_{h\nu}$ of $GeF_4^+ \tilde{D}\,^2A_1$.

To investigate the decay properties of the $\tilde{C}\,^2T_2$ state of GeF_4^+, the VUV radiation has been tuned through the $\tilde{C}$ state threshold at 18.52 eV. If the $\tilde{C}$ state decays radiatively, then from photoelectron data[15] $\tilde{C}$–$\tilde{X}$ and $\tilde{C}$–$\tilde{A}$ fluorescence is expected around 504 and 623 nm, respectively. However, no turn on in fluorescence in any wavelength region between 250 and 750 nm is observed. Thus, as with $SiF_4^+ \tilde{C}$, we conclude that $GeF_4^+ \tilde{C}$ decays nonradiatively by (pre)dissociation to fragments.

D. CCl_4

Neither $\tilde{C}\,^2T_2$ nor $\tilde{D}\,^2A_1$ states of CCl_4^+ decay radiatively.[4] Thus no sharp increase in fluorescence is observed when the ionizing radiation is tuned through the $\tilde{C}$ and $\tilde{D}$ thresholds of 16.7 and 20.4 eV. These experiments are described in Sec. IV of the previous paper.[4]

E. $SiCl_4$

The fluorescence spectrum between 14 and 35 eV is shown in Fig. 3 of the previous paper, and details are given in Sec. IV. In summary, the $\tilde{C}\,^2T_2$ state of $SiCl_4^+$ decays radiatively via bound–free $\tilde{C}$–$\tilde{X}$ and $\tilde{C}$–$\tilde{A}$ emission, but the $\tilde{D}\,^2A_1$ state does not fluoresce. Since partial ionization cross sections of the five valence molecular orbitals of $SiCl_4$ have been measured between 15 (the threshold for production of $SiCl_4^+ \tilde{C}$) and 80 eV,[35] it is possible to estimate $\phi_{h\nu}$ of $SiCl_4^+ \tilde{C}$. Thus between 16 and 34 eV $\phi_{h\nu} = 0.2$ and is independent of excitation energy. The uncertainty is as high as a factor of 2.

F. $GeCl_4$

The fluorescence spectrum between 14 and 35 eV is shown in Fig. 4 of the previous paper.[4] As with $SiCl_4$, the $\tilde{C}$ state of $GeCl_4^+$ decays radiatively, but the $\tilde{D}$ state does not. Partial ionization cross sections of the valence molecular or-

bitals of $GeCl_4$ have not been measured, and so it is not possible to estimate the fluorescence quantum yield of $GeCl_4^+ \tilde{C}$.

V. RADIATIVE LIFETIMES OF FLUORESCING STATES OF MX_4^+

In the single bunch mode, the Daresbury SRS is a pulsed source of electromagnetic radiation giving 200 ps wide pulses every 320 ns. It is an ideal source for measuring lifetimes in the range 1–50 ns, and since the repitition rate is so high lifetime decays can be accumulated very rapidly. We have measured the radiative lifetime τ of fluorescing states of MX_4^+ as a function of excitation energy. Since $\tau^{-1} = k_r + k_{nr}$ any variation in τ with energy can be ascribed to a change in the nonradiative decay rate k_{nr}, and hence a variation in $\phi_{h\nu}$ ($= k_r/k_r + k_{nr}$). All lifetimes were measured with a fast cooled Mullard 2020Q pm tube which is known to have excellent timing properties. In order to ensure that the decays were not distorted by space charge repulsion of the ions out of the observation region of the detector,[36,37] decays were measured over a range of pressures. The lifetimes are invariant to pressure over the range 10^{-5}–10^{-4} Torr, hence they are not limited by the space–charge effect.

A. CF_4

The photon count rate of $CF_4^+ \tilde{D}$–$\tilde{A},\tilde{B}$ is so low that it is not possible to measure the radiative lifetime of $CF_4^+ \tilde{D}\,^2A_1$. The $\tilde{C}\,^2T_2$ state lifetime has been measured using the Schott UG11 filter to isolate $CF_4^+ \tilde{C}$–$\tilde{X},\tilde{A}$ emission. Lifetimes were measured at nine excitation energies between 21.7 (threshold) and 30 eV. All decays fit to single exponentials, and the results are shown in Table II. The lifetime falls from 9.7 ns at threshold to 8.6 ns when the energy is 3 eV above threshold, then rises again to 9.0 ns at 8 eV above threshold. This variation is attributed to a change in the nonradiative decay rate k_{nr} as the excitation energy changes, and hence a change in $\phi_{h\nu}$. These results are in semiquantitative agreement with the measurement of $\phi_{h\nu}$ (Sec. IV A), where $\phi_{h\nu}$ falls by $\sim$30% between threshold and 5 eV above threshold, then rises again. Our lifetime values are in excellent agreement with the results of Hesser and Dressler,[38] who measured the radiative lifetime of the bands between 220 and 300 nm produced by 200 eV electron excitation of CF_4 to be 9.0 (9) ns.

TABLE II. Radiative lifetime of $CF_4^+ \tilde{C}\,^2T_2$ as a function of excitation energy.

E(eV)	λ(nm)[a]	τ(ns)[b]
21.9	56.5	9.66 (5)
22.3	55.5	9.35 (5)
22.7	54.5	8.75 (3)
23.6	52.5	8.58 (2)
24.5	50.5	8.61 (3)
25.6	48.5	8.59 (3)
26.6	46.5	8.65 (3)
27.8	44.5	8.84 (5)
29.2	42.5	8.96 (5)

[a] The resolution of the Seya monochromator is 0.5 nm.
[b] The number in parentheses indicates one standard deviation in the last digit.

The broad bands were unassigned by them, but are now known to be due to $CF_4^+ \tilde{C}$–$\tilde{X},\tilde{A}$. We note that they also measured the radiative lifetime of $CF_4^+ \tilde{D}$ to be 2.1 (2) ns. Both their lifetimes were cascade free, and this agrees with our observation that the decays obtained in this work are single exponential.

B. SiF_4

The radiative lifetime of the $\tilde{D}\,^2A_1$ state of SiF_4^+ has been measured using the Schott UG11 filter to isolate $SiF_4^+ \tilde{D}$–$\tilde{A},\tilde{B}$ emission. Measurements are made at 13 excitation energies between 21.5 (threshold) and 35 eV. The decays are all single exponential, and we measure $\tau = 9.30$ (4) ns and invariant to energy. This agrees with Hesser and Dressler's observation of cascade free decays with a lifetime of 10.4 (1.0) ns for the same emission bands.[38] The invariance of τ confirms the observation that $\phi_{h\nu}(SiF_4^+ \tilde{D})$ does not change with excitation energy (Sec. IV B).

C. GeF_4

The radiative lifetime of the $\tilde{D}\,^2A_1$ state of GeF_4^+ has been measured at three excitation energies of 21.7, 22.5, and 26.4 eV, using the Schott UG5 filter to isolate $GeF_4^+ \tilde{D}$–$\tilde{A},\tilde{B}$ fluorescence. [These decays were recorded before the cw fluorescence spectrum of GeF_4 had been obtained in detail; with hindsight we would have measured the lifetime at 24.4 eV (see Fig. 3).] It is not possible to fit the decay curves to single exponentials, but a double exponential fits all three curves well. Thus we obtain $\tau_1 = 3.1$ (3) ns and $\tau_2 = 6.3$ (4) ns for all three decays. This is the first observation of the radiative lifetime(s) of this state.

D. $SiCl_4$

The radiative lifetime of the $\tilde{C}$ state of $SiCl_4^+$ has been measured at six excitation energies between 15.1 (threshold) and 26 eV, using the Wratten 35 filter to isolate $SiCl_4^+ \tilde{C}$–$\tilde{X}$ fluorescence. One measurement was made at 16.6 eV corresponding to the Rydberg state of $SiCl_4$ between the $\tilde{C}$ and $\tilde{D}$ state ionization thresholds (see Sec. V C of Ref. 4). The decays are all single exponential, and we measure $\tau = 38.4$ (1) ns and invariant to energy. This is the first observation of the radiative lifetime of this state. The invariance of τ with energy confirms the observation that $\phi_{h\nu}$ ($SiCl_4^+ \tilde{C}$) is also constant with energy (Sec. IV E).

E. $GeCl_4$

The radiative lifetime of the $\tilde{C}$ state of $GeCl_4^+$ has been measured at four excitation energies between 14.5 (threshold) and 22 eV, using the Oriel LF42 filter to isolate $GeCl_4^+ \tilde{C}$–$\tilde{X}$ fluorescence. The decays are single exponential, with $\tau = 65.4$ (4) ns and invariant with energy. Again, this is the first observation of the radiative lifetime of this state. In conclusion, the lifetimes of the fluorescing states of MX_4^+ are collected together in Table III.

VI. DISCUSSION

In this and the previous paper, experiments have been described to probe the dynamics of the decay pathways of

TABLE III. Radiative lifetimes of fluorescing states of MX_4^+.

Ion	Electronic state	τ(ns)
CF_4^+	$\tilde{D}\,^2A_1$	2.1[a]
	$\tilde{C}\,^2T_2$	9.7–8.6[b]
SiF_4^+	$\tilde{D}\,^2A_1$	9.3
GeF_4^+	$\tilde{D}\,^2A_1$	3.1 and 6.3[c]
$SiCl_4^+$	$\tilde{C}\,^2T_2$	38.4
$GeCl_4^+$	$\tilde{C}\,^2T_2$	65.4

[a] Reference 38.
[b] Details in Table II.
[c] Biexponential decay.

the $\tilde{C}\,^2T_2$ and $\tilde{D}\,^2A_1$ excited electronic states of MX_4^+. We now attempt to rationalize these dynamic properties (a) with respect to their spectroscopic properties, and (b) with respect to the dissociation channels of MX_4^+.

(1) If the radiative lifetime τ is invariant to energy, then $\phi_{h\nu}$ of that state is constant. For SiF_4^+ $\tilde{D}$ τ is constant, $\phi_{h\nu}$ is close to unity, and thus there is no nonradiative decay channel. There is no "communication" between this state and the $SiF_2^+ + F_2$ and $SiF_3^+ + F$ dissociation channels which are energetically accessible. For CF_4^+ $\tilde{C}$ $\phi_{h\nu}$ is close to unity at threshold but decreases by $\sim 30\%$ as the energy is increased. We comment that three ionic dissociation channels lie within 1.6 eV above the $\tilde{C}$ threshold, and the decrease in $\phi_{h\nu}$ (corresponding to the small change in τ) could be rationalized by an increase in k_{nr} to one or more of these channels. For $SiCl_4^+$ $\tilde{C}$ τ is invariant to energy, but $\phi_{h\nu}$ is estimated to be as low as 0.2. This is surprising, since $\phi_{h\nu}$ would be expected to be close to unity for this state. We comment that this is not the ideal experiment to measure a fluorescence quantum yield, and a coincidence experiment (e.g., using the PIFCO technique[39,40]) would be more accurate.

(2) The biexponential decay behavior of GeF_4^+ $\tilde{D}$ is surprising, and suggests that the ions may not be produced by a direct photoionization process. However, this is in contradiction with the sharp turn on in the fluorescence signal at the $\tilde{D}$ state threshold (Fig. 3). We suspect that the decay properties are related to the unassigned peaks in the excitation spectrum above the $\tilde{D}$ threshold (Sec. IV C), but as yet we do not know how. The results suggest that there may be a second emitter other than GeF_4^+ fluorescing in the UV and visible. Dispersion of the fluorescence in the cw mode of the synchrotron, and time-gated fluorescence detection in the pulsed mode might help to clarify the situation.

(3) There is a clear connection between the spectroscopic and dynamic properties of the $\tilde{C}\,^2T_2$ state of the three fluorides which cannot be coincidental. CF_4^+ $\tilde{C}$ does not show Jahn–Teller distortion from tetrahedral symmetry,[1] and this state decays radiatively; SiF_4^+ and GeF_4^+ $\tilde{C}$ do distort from T_d geometry,[2,3] and now the nonradiative decay pathway is operative. As mentioned in the previous paper, it would be interesting to see if this connection is apparent with the chlorides, i.e., to observe the presence or absence of Jahn–Teller activity in CCl_4^+, $SiCl_4^+$, and $GeCl_4^+$ $\tilde{C}\,^2T_2$.

(4) These experiments have only monitored the radiative decay channel of the $\tilde{C}$ and $\tilde{D}$ states of the parent molecular ion. To build up a complete picture of the dynamics, the nonradiative decay channel needs to be monitored simultaneously. Thus if $\phi_{h\nu} < 1$ we need to measure which fragment ions are produced as a function of excitation energy (using a time-of-flight mass analyzer). Such experiments are being planned.

ACKNOWLEDGMENTS

We thank the staff of the Daresbury Laboratory (especially Dr. D. M. P. Holland, Dr. D. A. Shaw, and Dr. J. B. West) for their help and advice with the experiments. We thank Dr. A. J. Edwards and Mr. K. Greenwood (Birmingham University) for preparing the GeF_4, and Dr. L. A. Chewter (Shell Thornton Research Centre) for the use of his multiexponential fitting program. The financial support of SERC is acknowledged. I. R. L. and S. M. M. thank SERC and the University of Cambridge (Sims Scholarship), respectively, for Research Studentships.

[1] J. F. M. Aarts, S. M. Mason, and R. P. Tuckett, Mol. Phys. **60**, 761 (1987).
[2] S. M. Mason and R. P. Tuckett, Mol. Phys. **60**, 771 (1987).
[3] S. M. Mason and R. P. Tuckett, Mol. Phys. **62**, 979 (1987).
[4] I. R. Lambert, S. M. Mason, R. P. Tuckett, and A. Hopkirk, J. Chem. Phys. **89**, 2675 (1988).
[5] J. F. M. Aarts, Chem. Phys. Lett. **114**, 114 (1985).
[6] J. F. M. Aarts, Chem. Phys. **101**, 105 (1986).
[7] H. van Lonkhuyzen and J. F. M. Aarts, Chem. Phys. Lett. **140**, 434 (1987).
[8] S. M. Mason and R. P. Tuckett, Mol. Phys. **62**, 175 (1987).
[9] L. C. Lee, J. Phys. B **10**, 3033 (1977).
[10] J. H. D. Eland, M. Devoret, and S. Leach, Chem. Phys. Lett. **43**, 97 (1976).
[11] C. R. Brundle, M. B. Robin, and H. Basch, J. Chem. Phys. **53**, 2196 (1970).
[12] R. Jadrny, L. Karlsson, L. Mattsson, and K. Siegbahn, Chem. Phys. Lett. **49**, 203 (1977).
[13] D. R. Lloyd and P. J. Roberts, J. Electron. Spectrosc. **7**, 325 (1975).
[14] H. van Lonkhuyzen (private communication).
[15] S. Cradock, Chem. Phys. Lett. **10**, 291 (1971).
[16] H. van Lonkhuyzen and C. A. de Lange, Chem. Phys. **89**, 313 (1984).
[17] C. E. Moore, *Atomic Energy Levels*, Natl. Stand. Ref. Data Ser., Natl. Bur. Stand. Circ. No. 467 (U. S. GPO, Washington, D. C., 1949).
[18] G. Herzberg and K. P. Huber, *Constants of Diatomic Molecules* (Van Nostrand, Reinhold, New York, 1979).
[19] *JANAF Thermochemical Tables*, Natl. Stand. Ref. Data Ser., Natl. Bur. Stand. Circ. No. 37 (U. S. GPO, Washington, D. C., 1971).
[20] R. Walsh, Acc. Chem. Res. **14**, 246 (1981).
[21] P. W. Harland, S. Cradock, and J. C. J. Thynne, Int. J. Mass Spectrom. Ion Phys. **10**, 169 (1972).
[22] J. M. Dyke, A. E. Lewis, and A. Morris, J. Chem. Phys. **80**, 1382 (1984).
[23] G. Bosser, H. Bredohl, and I. Dubois, J. Mol. Spectrosc. **106**, 72 (1984).
[24] F. Melen and I. Dubois, J. Mol. Spectrosc. **124**, 476 (1987).
[25] J. M. Dyke, L. Golab, N. Jonathan, A. Morris, and M. Okuda, J. Chem. Soc. Faraday Trans. 2 **70**, 1828 (1974).
[26] N. P. C. Westwood, Chem. Phys. Lett. **25**, 558 (1974).
[27] K. F. Zmbov, J. W. Hastie, R. Hauge, and J. L. Margrave, Inorg. Chem. **7**, 608 (1968).
[28] C. Lifshitz and W. A. Chupka, J. Chem. Phys. **47**, 3439 (1967).
[29] J. D. McDonald, C. H. Williams, J. C. Thompson, and J. L. Margrave, Adv. Chem. Ser. **72**, 261 (1968).
[30] L. C. Lee, E. Phillips, and D. L. Judge, J. Chem. Phys. **67**, 1237 (1977).
[31] T. A. Carlson, A. Fahlman, W. A. Svensson, M. O. Krause, T. A. Whitley, F. A. Grimm, M. N. Piancastelli, and J. W. Taylor, J. Chem. Phys. **81**, 3828 (1984).
[32] L. C. Lee, X. Wang, and M. Suto, J. Chem. Phys. **85**, 6294 (1986).
[33] B. W. Yates, K. H. Tan, G. M. Bancroft, L. L. Coatsworth, and J. S. Tse, J. Chem. Phys. **83**, 4906 (1985).

[34]M. Suto, X. Wang, L. C. Lee, and T. J. Chuang, J. Chem. Phys. **86**, 1152 (1987).
[35]T. A. Carlson, A. Fahlman, M. O. Krause, T. A. Whitley, F. A. Grimm, M. W. Piancastelli, and J. W. Taylor, J. Chem. Phys. **84**, 641 (1986).
[36]L. J. Curtis and P. Erman, J. Opt. Soc. Am. **67**, 1218 (1977).
[37]G. R. Mohlmann and F. J. de Heer, Phys. Scr. **16**, 51 (1977).
[38]J. E. Hesser and K. Dressler, J. Chem. Phys. **47**, 3443 (1967).
[39]G. Dujardin, S. Leach, and G. Taieb, Chem. Phys. **46**, 407 (1980).
[40]R. P. Tuckett, E. Castellucci, M. Bonneau, G. Dujardin, and S. Leach, Chem. Phys. **92**, 43 (1985).
[41]We comment that our definition of $\phi_{h\nu}$ (the ratio of the radiative decay rate of $CF_4^+\ \tilde{C}$ to the sum of the radiative and nonradiative rates) differs from that which Lee *et al.* call the fluorescence quantum yield. Their's is the ratio of the fluorescence cross section to the total absorption cross section, where the fluorescence cross section is the partial ionization cross section into $CF_4^+\ \tilde{C}(\sigma)\times\phi_{h\nu}$. Thus they measure a fluorescence quantum yield of 0.25 at 23 eV (Fig. 6 of Ref. 32) where the partial ionization and absorption cross sections are 12.6 and 64.2 Mb, respectively (Ref. 31). Hence $\phi_{h\nu} = 1.3$. We believe that our definition of $\phi_{h\nu}$ is more applicable to this work, and it is the one used throughout this paper.